

## Microstructural evolution and fracture toughness of Al<sub>2</sub>O<sub>3</sub>/Ti composites

M. Vázquez-Villar, M. Romero-Romo, A. Altamirano-Torres and E. Rocha-Rangel\*

Departamento de Materiales, Universidad Autónoma Metropolitana Av. San Pablo No. 180, Col. Reynosa-Tamaulipas, México, D. F. 02200, México

The effect of different additions of a metal (Ti) on the microstructure and fracture toughness of Al<sub>2</sub>O<sub>3</sub>-based ceramics, as well as the establishment of a route for their processing was analyzed in this study. The samples were prepared by means of mechanical milling and pressureless sintering in an argon atmosphere. Due to the fact of working with very small sizes of powders of both the metal and ceramic, it was possible to reach in sintered products greater values of densification than 95% of their relative density. Measurements of fracture toughness ( $K_{IC}$ ) evaluated by the fracture indentation method, indicate that this mechanical property had improved with some additions of Ti in the composite, for example  $K_{IC}$  for pure alumina processed under the conditions of this study was 3.0 MPa·m<sup>1/2</sup>, whereas,  $K_{IC}$  for the composite with 3 vol % Ti was 4.1 MPa·m<sup>1/2</sup>. The microstructure observed in a scanning electron microscopy shows the formation of small and fine metallic interpenetrating networks in the ceramic matrix, that improve in their formation with an increases of Ti in the composite.

**Key words:** Al<sub>2</sub>O<sub>3</sub>/Ti Composites, Microstructural evolution, Fracture toughness.

### Introduction

Recently, interpenetrating composites of ceramics and metals have been designed to take advantage of the best properties of both phases. High wear resistance is achieved from ceramic/metal microstructures because of the high hardness and high wear resistance of the ceramic fraction of the composite. The metallic fraction increases the fracture toughness of the composite, which improves its damage tolerance. Interpenetrating composites have an advantage over other types, because the continuous metallic network provides dimensional stability at high temperatures [1, 2]. Interpenetrating ceramic/metal composites can be fabricated by a number of techniques: by direct oxidation of a metal [3], by metal infiltration of a ceramic perform both with [4] and without external pressure [5], by reactive metal penetration [6, 7] and by hot pressing [8]. For example, Ni<sub>3</sub>Al/Al<sub>2</sub>O<sub>3</sub> composites produced via pressure infiltration into a presintered Al<sub>2</sub>O<sub>3</sub> body have shown high fracture toughness (12 MPa·m<sup>1/2</sup>), even at temperatures of 800 °C [9]. These alumina/aluminide alloy (3A) composites are of particular interest for their high melting points, low overall densities, and good corrosion and oxidation resistance. However, most of these processes are expensive, present low productivity and they are difficult in their operation. Therefore, simple and cheaper processes are now in development for the production of larger amounts of ceramic/metal composites. High-energy ball milling

is an alternative, low-cost method for the production of ceramic/metal composites, and conventional powder-techniques can be applied for forming and densification. Milling can be performed under vacuum, air or inert atmosphere as well as under dry or wet conditions, using an organic milling agent [10], in addition, it allows for a variation of the metallic phase or the ceramic volume fraction over a wide range. In this way, the properties of the composite can be tailored to suit the desired application.

In this paper, examples of microstructural evolution during processing are presented and results of mechanical property measurement are compared to monolithic Al<sub>2</sub>O<sub>3</sub>.

### Experimental Procedure

The starting materials were Al<sub>2</sub>O<sub>3</sub> powder (99.9%, 1 μm, Sigma, U.S.A.) and Ti powder (99.9%, 1-2 μm, Aldrich, U.S.A.). The final titanium contents in the composites produced were 0, 0.5, 1, 2, 3 and 10 vol %. Powder blends of 50 g were prepared in a ball mill; the rotation speed of the mill was at maximum intensity (300 rpm) for a duration up to 12 h, using 500 g ZrO<sub>2</sub> balls and a 1000 ml Al<sub>2</sub>O<sub>3</sub> vial. With the milled powder mixture, green cylindrical compacts 2 cm diameter and 0.2 cm thickness were fabricated by uniaxial pressing using 270 MPa pressure. Then pressureless sintering was performed under an argon flux of 10 cm<sup>3</sup>/minute and at a temperature of 1500 °C. Densities of sintered specimens were determined using the Archimedes method. The microstructure was observed by optical microscopy (OM) and scanning electron microscopy (SEM). The hardness of samples was evaluated as micro-hardness using a Vickers indentation, using 500 g

\*Corresponding author:  
Tel : +52-55-53-18-90-82  
Fax: + 52-55-53-82-39-98  
E-mail: rre@correo.azc.uam.mx

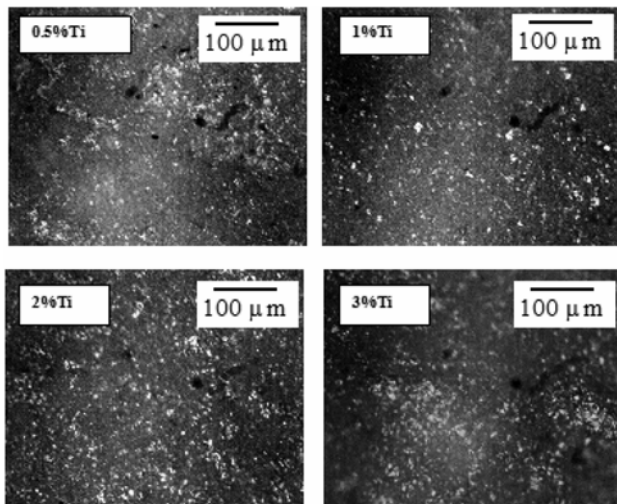


**Fig. 1.** Optical micrographs of manufactured composites as a function of the content of titanium.

load for 10 s, ten indents were made in each specimen to determine the average and standard deviation, fracture toughness was estimated by the fracture indentation method [11], and the elastic modulus was determined by an ultrasonic method.

## Results and Discussion

### Microstructure

Figure 1 shows optical micrographs of the different composites. In all the images there is the presence of two phases, a dark gray that corresponds to the ceramic matrix and a white that corresponds to the reinforcing metallic particles. Both phases are interconnected, forming a three-dimensional interpenetrating network throughout the microstructure. The phases appear to be homogeneously distributed. When the microstructure was observed by optical microscopy, no evidence of residual porosity or microcracking was obtained.

Figure 2 shows scanning electron micrographs taken from polished cross section of the different composites. Sufficiently refined and homogeneous microstructures are achieved in all samples. The ligament diameter ranges from about 1 to 3  $\mu\text{m}$  and it appears to be independent of the amount of titanium in the composite. The grain size of alumina ranges from 3 to 12  $\mu\text{m}$  and it appears to grow with increments of Ti in the composite. In these

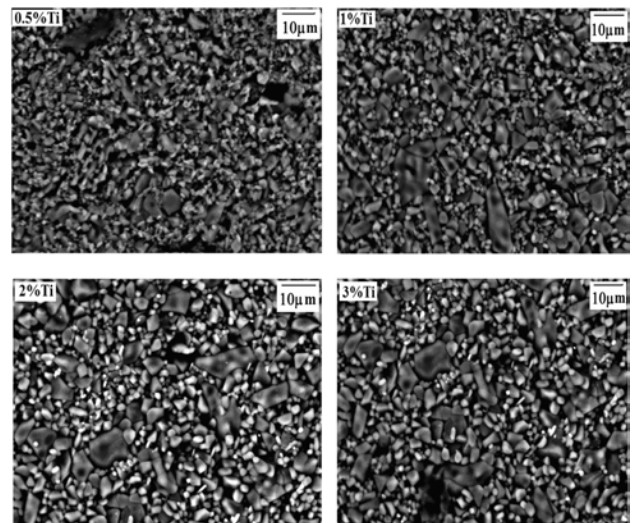


**Fig. 2.** Scanning electron micrographs of manufactured composites as a function of the content of titanium.

images it is possible to observe some porosity in the samples. In all samples, the alumina-matrix and reinforcing metal were identified with the help of EDS analysis performed during SEM observations, in this way gray particles were identified as the alumina-matrix, while, white and smaller particles were recognized as titanium. Table 1 reports the relative densities of the different composites after sintering, relative densities range between 94.73 to 99.20%, depending on the metal volume fraction in the composite.

Figure 3 shows both representative optical and scanning electron micrographs of a composite with a titanium content of 10 vol%. Here is most evidence for the formation of the metallic interpenetrating networks (clear and brightness phase) formed by the titanium used as the reinforced material of the ceramic matrix. This network surrounds effectively some ceramic grains of the matrix. In general the presence of a composite with a fine and homogenous microstructure is established.

### Mechanical properties

The values of the measurements of the mechanical properties evaluated in the materials made here are reported in Table 1. For all fracture toughness, Young's modulus and hardness measurements, both; mean value and the standard deviation are reported.

**Table 1.** Values of mechanical properties of the different studied materials

| Composite                      | Relative density (%) | Theoretical Young's modulus (GPa) | Experimental Young's modulus (GPa) | Micro-hardness (GPa) | Fracture toughness ( $\text{MPa}\cdot\text{m}^{1/2}$ ) |
|--------------------------------|----------------------|-----------------------------------|------------------------------------|----------------------|--|
| $Al_2O_3$                      | 94.95                | 380                               | 257 +/- 13                         | 1097 +/- 16          | 3.0 +/- 0.1  |
| $Al_2O_3/0.5 \text{ vol \%Ti}$ | 94.73                | 379                               | 263 +/- 12                         | 1050 +/- 15          | 3.2 +/- 0.2  |
| $Al_2O_3/1 \text{ vol \%Ti}$   | 96.32                | 376                               | 266 +/- 13                         | 1045 +/- 16          | 3.6 +/- 0.1  |
| $Al_2O_3/2 \text{ vol \%Ti}$   | 97.93                | 373                               | 272 +/- 11                         | 1042 +/- 15          | 3.9 +/- 0.1  |
| $Al_2O_3/3 \text{ vol \%Ti}$   | 97.98                | 369                               | 274 +/- 12                         | 1035 +/- 16          | 4.1 +/- 0.1  |
| $Al_2O_3/10 \text{ vol \%Ti}$  | 99.20                | 354                               | 301 +/- 12                         | 917 +/- 12           | 3.7 +/- 0.1  |

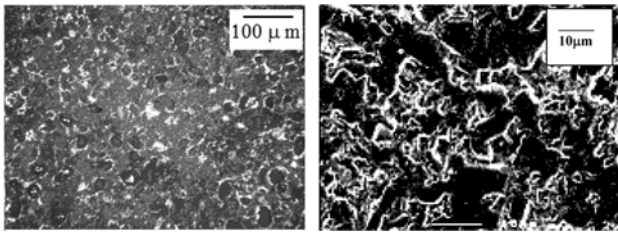


**Fig. 3.** Optical and scanning electron micrographs of a composite with a titanium content of 10 vol %.

### Fracture toughness

Fracture toughness of the composites is plotted as a function of metal content in Fig. 4. The results of mechanical tests show that the fracture toughness is enhanced when in the microstructure of the composite there is the presence of a ductile metal. In this way the fracture toughness have been improved by 7, 19, 29, 38 and 23% for samples with 0.5, 1, 2, 3 and 10 vol% Ti respectively. This observation may be due to plastic deformation of the metallic phase, which forms crack-bridging ligaments, as has been reported before by several authors [4, 9, 12].

### Young's moduli

Young's moduli of the composites are plotted as a function of metal content in Fig. 5. Reported on the same

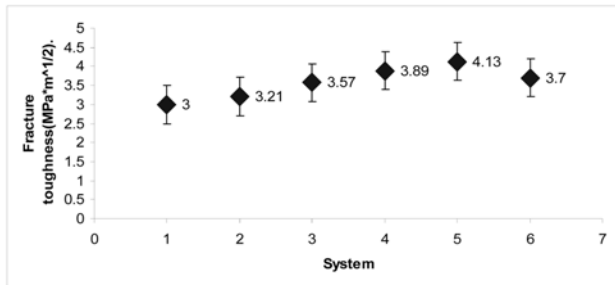


**Fig. 4.** Fracture toughness of different systems after sintering at 1500 °C for 1 h. 1- $\text{Al}_2\text{O}_3$ , 2- $\text{Al}_2\text{O}_3/0.5$  vol%Ti, 3- $\text{Al}_2\text{O}_3/1$  vol%Ti, 4- $\text{Al}_2\text{O}_3/2$  vol%Ti, 5- $\text{Al}_2\text{O}_3/3$  vol%Ti and 6- $\text{Al}_2\text{O}_3/10$  vol%Ti.

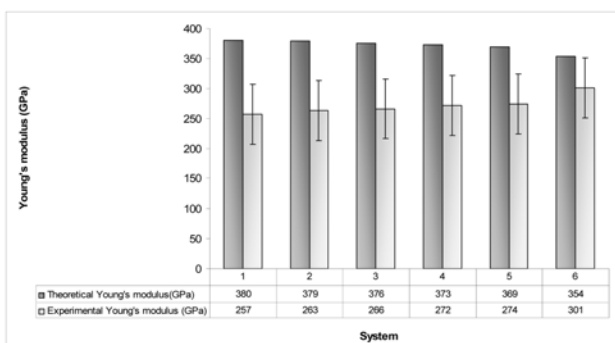


**Fig. 5.** Theoretical and experimental Young's modulus of different systems after sintering. Dark bars correspond to theoretical values; clear bars correspond to experimental values. 1- $\text{Al}_2\text{O}_3$ , 2- $\text{Al}_2\text{O}_3/0.5$  vol%Ti, 3- $\text{Al}_2\text{O}_3/1$  vol%Ti, 4- $\text{Al}_2\text{O}_3/2$  vol%Ti, 5- $\text{Al}_2\text{O}_3/3$  vol%Ti and 6- $\text{Al}_2\text{O}_3/10$  vol%Ti.

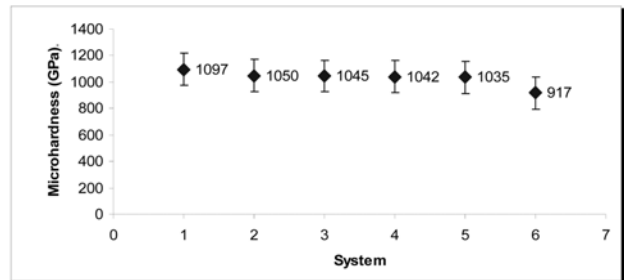


**Fig. 6.** Microhardness of different systems after sintering at 1400 °C for 1 h. 1- $\text{Al}_2\text{O}_3$ , 2- $\text{Al}_2\text{O}_3/0.5$  vol%Ti, 3- $\text{Al}_2\text{O}_3/1$  vol%Ti, 4- $\text{Al}_2\text{O}_3/2$  vol%Ti, 5- $\text{Al}_2\text{O}_3/3$  vol%Ti and 6- $\text{Al}_2\text{O}_3/10$  vol%Ti.

figure are theoretical estimates of Young's modulus given by the rule of mixtures. The data collected in this study clearly lie below the theoretical predictions. The difference between both values of Young's modulus is due to the remaining porosity in each composite after the sintering stage.

### Microhardness

The measured micro-hardness of the samples as a function of titanium content in the composites are plotted in Fig. 6. In this figure it is seen that the micro-hardness of the composites diminish with increments of the titanium fraction in the composite. This behavior is logical because titanium is softer than alumina, so when it is incorporated in an alumina ceramic matrix its presence diminishes its hardness.

### Conclusions

$\text{Al}_2\text{O}_3/\text{Ti}$  composites with interpenetrating network microstructures can be manufactured by a combination of mechanical milling and pressureless sintering of  $\text{Al}_2\text{O}_3$  and Ti mixture powders.

Homogeneous  $\text{Al}_2\text{O}_3$ -based composites with a fracture toughness as high as  $4.1 \text{ MPa} \cdot \text{m}^{1/2}$  for the composite with 3 vol% Ti could be obtained, also they show better damage tolerance than does monolithic  $\text{Al}_2\text{O}_3$ .

The refined and homogeneous incorporation of a ductile metal (Ti) in a hard ceramic matrix ( $\text{Al}_2\text{O}_3$ ) improves its fracture toughness.

### Acknowledgments

Authors thankfully acknowledge the Departamento de Materiales at UAM-A, for financial assistance through project 2260235. Also we acknowledge the help of Dr. Eduardo Terrés from The Laboratorio de Microscopía Electrónica de Ultra Alta Resolución, Instituto Mexicano del Petróleo for the SEM analysis of the samples. ERR and MRR acknowledges the support of the SNI-Conacyt.

### References

1. C.J. McMahon, Jr. in Structural Materials, Merion Books, Philadelphia, PA (2004) 315-348.

2. J.K. Wessel, in *The Handbook of Advanced Materials*, John Wiley & Sons, New Jersey (2004) 66-88.
3. M.S. Newkirk, A.W. Urquhart, H.R. Zwickler and E. Breval, *J. Mater. Res.* 1 (1986) 81-89.
4. S. Wu, A.J. Gesing, N.A. Travitzky and N. Claussen, *J. Eur. Ceram. Soc.* 7 (1991) 277-281.
5. C. Toy and W.D. Scott, *J. Am. Ceram. Soc.* 73 (1990) 97-101.
6. S.M. Naga, A. El-Maghraby and A.M. El-Rafei, *Am. Ceram. Bull.* 86 (2007) 9301-9307.
7. R.E. Loehman, K. Ewsuk and P. Tomsia, *J. Am. Ceram. Soc.* 79 (1996) 27-32.
8. E. Rocha and C. Vilchis, in *Proceedings of 5th International Conference on High-Temperature Ceramic Matrix Composites-HTCMC5*, American Ceramic Society, Westerville, OH (2004) 347-352.
9. J. Rodel, H. Prielipp, N. Claussen, M. Sternitzke, K.B. Alexander, P.F. Becher and J.H. Schneibel, *Scr. Met. Mater.* 33 (1995) 843-848.
10. N. Claussen, D.E. Garcia and R. Janssen, *J. Mater. Res.* 11 (1996) 2884-2888.
11. A.G Evans and E.A. Charles, *J. Am. Ceram. Soc.* 59 (1976) 371-372.
12. T. Klassen, R. Gunther, B. Dickau, F. Gartner, A. Bartels, R. Bormann and H. Mecking, *J. Am. Ceram. Soc.* 81 (1998) 2504-2506.